"Unexpected" ^{29}Si NMR Chemical Shifts in Heteroatom-Substituted Silyllithium Compounds: A Quantum-Chemical Analysis

Dominik Auer, Martin Kaupp,* and Carsten Strohmann*

Institut für Anorganische Chemie, Universität Würzburg, Am Hubland, 97074 Würzburg, Germany

Received March 15, 2004

Previous ^{29}Si NMR spectroscopic investigations of various heteroatom-substituted silyllithium compounds revealed "unexpectedly" high silicon chemical shifts. To find explanations for these observations, the ^{29}Si chemical shift tensors of various methoxy-, dimethylamino-, and methylthio-substituted chloro and lithiosilanes have been evaluated by quantum-chemical calculations. Substituent effects on shielding have been analyzed by IGLO-DFT calculations. Popular notions on the influence of atomic charge and substituent electronegativity on the central-atom shifts are not applicable. The combination of very electronegative and electropositive substituents leads to large deshielding contributions in heteroatom-substituted silyllithium compounds. As shown by analyses of localized molecular orbital (LMO) contributions to shielding, this is due to a coupling of bonding and antibonding orbitals with large silicon character and small energy differences. After a comparison of IGLO-LMO results and GIAO-based natural chemical shielding analyses, the LMO interpretations have been augmented further by an inspection of natural bond orbitals, to provide a consistent interpretation of the substituent effects on chemical shifts. The presented results should be transferable also to other heteroatom-substituted p-block main-group compounds.

1. Introduction

Lithiated silanes are useful and important reagents for the transfer of silyl groups to organic and organometallic systems.[1,2] Due to their very special routes of preparation (cleavage of disilanes or reaction of chlorosilanes with lithium; metal−lithium exchange reactions, e.g. starting from stannosilanes)[3] only a restricted variety of compounds has been obtained so far. These are mostly limited to (alkylsilyl)- and (arylsilyl)lithiums, whereas functionalized silyllithium species such as alkoxy-, dialkylamino-, or organylthio-substituted systems are rare.[4−7]

To probe the geometric and electronic structures of these highly reactive molecules, ^{29}Si NMR spectroscopy has proven to be the method of choice. Several experimental investigations of exclusively aryl- and alkyl-substituted silyllithiums by ^{29}Si NMR spectroscopy have indicated, as expected, significantly lower values of the chemical shift (CS) compared to those of the corresponding chlorosilanes (see Figures 1 and 2 for examples).[7] However, the situation becomes complicated when alkyl or aryl groups are exchanged for heteroatom substituents. For chlorosilanes, the ^{29}Si NMR resonances change significantly to higher field.[4,7] This is inconsistent with widespread notions on deshielding by charge transfer from silicon to electronegative substituents. Such simplified arguments based on atomic charge[4,7] are even less suitable for heteroatom-substituted silyllithiums, where the ^{29}Si resonances are shifted tremendously to lower field compared to the corresponding chlorosilane systems (see Figures 1 and 2 for selected molecules and ^{29}Si shifts).

Quantum-chemical analyses should provide a better understanding and hopefully could render the ^{29}Si shifts a reliable tool for the characterization of structure and bonding of silyllithium species.[8] Preliminary theoretical studies of the unexpected downfield chemical shifts in the ^{29}Si NMR of amino-functionalized silyllithium compounds have been reported recently.[2] Here we provide a full, systematic investigation of dimethylamino-, methoxy-, and methylthio-substituted systems.

2. Theoretical Background

The proper starting point for an analysis of the origin of the chemical shifts is Ramsey's second-order pertur-

* To whom correspondence should be addressed. E-mail: mail@carsten-strohmann.de (C.S.); kaupp@mail.uni-wuerzburg.de (M.K.).

(1) (a)Fleming, I. In *Organocopper Reagents*; Taylor, R. J. K., Ed.; Oxford University Press: Oxford, U.K., 1994; p 257. (b) Fleming, I.; Roberts, R. S.; Smith, S. C. *J. Chem. Soc., Perkin Trans. 1* **1998**, 1209. (c) Fleming, I.; Roberts, R. S.; Smith, S. C. *J. Chem. Soc., Perkin Trans. 1* **1998**, 1215. (d) Schubert, U.; Schenkel, A. *Transition Met. Chem.* **1985**, *10*, 210. (e) Strohmann, C.; Hörnig, J.; Auer, D. *Chem. Commun.* **2002**, 766.

(2) Strohmann, C.; Ulbrich, O.; Auer, D. *Eur. J. Inorg. Chem.* **2001**, 1013.

(3) (a) Lickiss, P. D.; Smith, C. M. *Coord. Chem. Rev.* **1995**, *145*, 75. (b) Tamao, K.; Kawachi, A. *Adv. Organomet. Chem.* **1995**, *38*, 1. (c) Sekiguchi, A.; Lee, V. Y.; Nanjo, M. *Coord. Chem. Rev.* **2000**, *210*, 11.

(4) Kawachi, A.; Tamao, K. *J. Am. Chem. Soc.* **2000**, *122*, 1919.

(5) Tamao, K.; Kawachi, A.; Ito, Y. *J. Am. Chem. Soc.* **1992**, *114*, 3989. Trommer, K.; Herzog, U.; Georgi, U.; Roewer, G. *J. Prakt. Chem.* **1998**, *340*, 557.

(6) Kawachi, A.; Tamao, K. 33rd Organosilicon Symposium, April 6−8, 2000; Saginaw, MI; PA 59.

(7) Kawachi, A.; Tamao, K. *Bull. Chem. Soc. Jpn.* **1997**, *70*, 945 and references cited therein.

(8) Kaupp, M. In *Calculation of NMR and EPR Parameters*, 1st ed.; Kaupp, M., Bühl, M., Malkin, V. G., Eds.; Wiley-VCH: Weinheim, Germany, 2004; p 291.

10.1021/om049812k CCC: $27.50
Publication on Web 06/16/2004

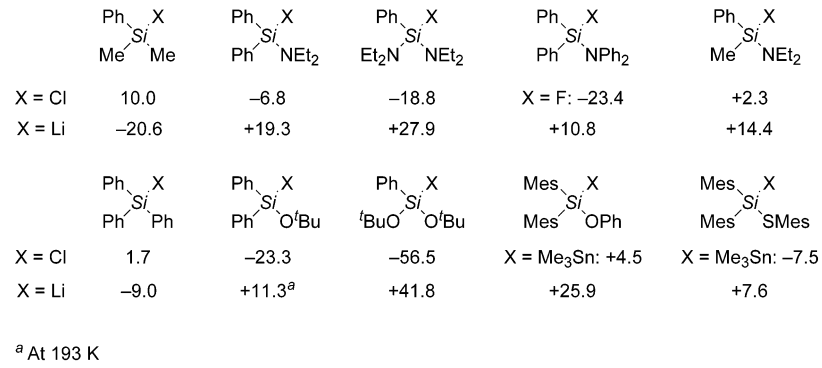

Figure 1. Experimentally determined ^{29}Si NMR shifts of selected silanes.[6,7]

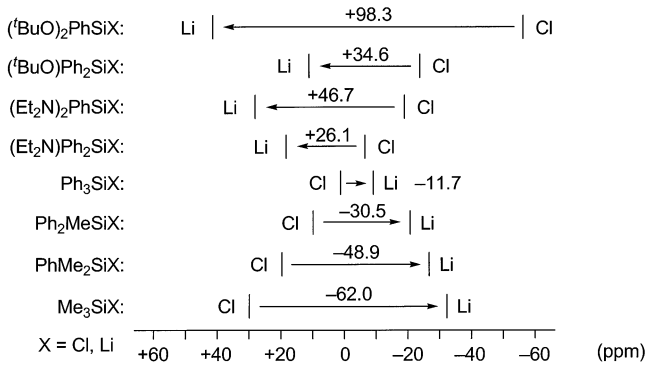

Figure 2. Changes in ^{29}Si shifts ($\Delta\delta$) from various chlorosilanes to the corresponding silyllithiums.

bation equations[9] (relativistic effects may provide further contributions in heavy-atom systems[10]). Except for proton NMR, it is usually assumed that changes in chemical shifts with different chemical environments are due to changes in the paramagnetic contribution to nuclear shielding, σ^{p}:[11]

$$\sigma_N{}^{p} = \frac{1}{2c^2}\sum_{n\neq 0}\frac{\langle\Psi_n|L_O|\Psi_0\rangle\cdot\langle\Psi_0|L_N\cdot r_N{}^{-3}|\Psi_n\rangle}{E_0 - {}^1E_n} + \text{cc} \quad (1)$$

Here, Ψ_0 and Ψ_n are the many-electron wave functions of the ground state and nth excited singlet state, respectively, and E_0 and ^1E_n provide the corresponding energies. The two matrix elements in the numerator reflect interactions with (a) the external magnetic field ("orbital Zeeman term"—OZ; left side) and (b) the magnetic moment of the nucleus in question (the "paramagnetic-nuclear-spin-electron-orbit term"—PSO;[11] right side).

When using a wave function Ψ_0 that consists of a single Slater determinant of molecular orbitals (MOs), as in Hartree–Fock or density functional theories, we may rewrite eq 1 as a double sum over occupied and virtual molecular orbitals ϕ_k and ϕ_a, respectively (with orbital energies ϵ_k and ϵ_a; u and v represent Cartesian components):[11]

$$\sigma_{N,uv}{}^{p} = \frac{2}{c^2}\sum_{k}^{occ}\sum_{a}^{vac}\frac{\langle\varphi_k|l_{O,u}|\varphi_a\rangle\cdot\langle\varphi_a|l_{N,v}\cdot r_N{}^{-3}|\varphi_k\rangle}{\epsilon_k - \epsilon_a} \quad (2)$$

In the case of local (LDA) or gradient-corrected (GGA) density functional calculations without current-dependent terms, an uncoupled DFT (UDFT[12]) approach results, whereas exchange coupling terms enter the PSO matrix elements in the case of Hartree–Fock or hybrid-DFT calculations and require an iterative solution of coupled-perturbed equations.[13] Our analysis in this work will be restricted to the BP86 functional[14] (which is a GGA functional) and thus to the more transparent UDFT treatment.

Equations 1 and 2 refer to a common gauge origin but can be extended to other choices of gauge.[13,15] Two of the most widely used distributed gauge methods are the gauge including atomic orbital (GIAO)[16] and individual gauge for localized orbital (IGLO)[17] approaches. While results obtained with the former have usually been analyzed in terms of canonical molecular orbitals (CMO), the latter are most suitably broken down in contributions from occupied localized MOs (LMOs) and virtual CMOs. This distinction is not mandatory, however, as unitary transformations of the molecular orbitals may be carried out for any chosen gauge. For example, Weinhold and co-workers have proposed "natural chemical shielding" (NCS) analysis, which involves an orbital transformation of GIAO shieldings, to give strictly localized natural bond orbital (NBO) or natural localized molecular orbital (NLMO) contributions.[18] While the overall shielding results will not depend on such unitary transformation of the orbitals and are not expected to differ much between GIAO and IGLO calculations, the interpretation of the shieldings will depend appreciably on the chosen set of orbitals. Furthermore, while single gauge origin (SGO) methods provide only diamagnetic "ground-state-like" and para-

(9) Ramsey, N. F. *Phys. Rev.* **1950**, *78*, 699.
(10) Kaupp, M.; Malkina, O. L.; Malkin, V. G.; Pyykkö, P. *Chem. Eur. J.* **1998**, *4*, 118.
(11) L_O represents angular momentum around the gauge origin of the external vector potential due to the external magnetic field, and L_N represents angular momentum around the nucleus in question. Both of these operators may be expressed as a sum over one-electron operators l_O and l_N, respectively. Equation 1 uses cgs-based atomic units, and c is the speed of light.
(12) Malkin, V. G.; Malkina, O. L.; Eriksson, L. A.; Salahub, D. R. In *Modern Density Functional Theory: A Tool for Chemistry*; Seminario, J. M., Politzer, P., Eds.; Elsevier: Amsterdam, The Netherlands, 1995; Vol. 2, p 273.
(13) Kutzelnigg, W.; Fleischer, U.; Schindler, M. In *NMR-Basic Principles and Progress*; Diehl, P., Fluck, E., Günther, H., Kosfeld, R., Eds.; Springer-Verlag: Heidelberg, Germany, 1990; Vol. 23, p 165.
(14) (a) Becke, A. D. *Phys. Rev. A* **1988**, *38*, 3098. (b) Perdew, J. P. *Phys. Rev. B* **1986**, *33*, 8822.
(15) Wolinski, K.; Hinton, J. F.; Pulay, P. *J. Am. Chem. Soc.* **1990**, *112*, 8251.
(16) Ditchfield, R. *Mol. Phys.* **1974**, *27*, 789.
(17) Kutzelnigg, W. *Isr. J. Chem.* **1980**, *19*, 193. Schindler, M.; Kutzelnigg, W. *J. Chem. Phys.* **1982**, *76*, 1919.
(18) Bohmann, J. A.; Weinhold, F.; Farrar, T. C. *J. Chem. Phys.* **1997**, *107*, 1173.

	IGLO/ LMO	GIAO/ CMO	SGO/ CMO	GIAO/ NCS (NBO,NLMO)
advantages	• clear interpretation in well localizable systems	• relation of energy denominators to UV/vis spectroscopy • CMOs suitable for delocalized systems	• no complication from σ^{p0} • relation of energy denominators to UV/vis spectroscopy	• good in well localizable systems • interpretation of small delocalization effects
disadvantages	• σ^{p0} not constant & hard to interpret • canonical virtual MOs • no relation of energy denominators to UV/vis spectroscopy	• σ^{p0} not constant & hard to interpret • CMOs do not provide simple relation to Lewis structures	• often poor quantitative results (basis set) • CMOs do not provide simple relation to Lewis structures	• no true relation of energy denominators to UV/vis spectroscopy • core-orbital contributions sometimes not transferable

Figure 3. Advantages and disadvantages of selected methods for the interpretation of nuclear shieldings.

magnetic "sum-over-states-like" contributions, σ^{d} and σ^{p}, respectively, distributed-gauge methods such as IGLO and GIAO introduce further method-specific couplings among the occupied orbitals (gauge terms), that we will in the following term σ^{p0}, in contrast to occupied-virtual couplings σ^{p1}. See ref 8 for a more detailed discussion of these issues. Figure 3 summarizes briefly the possible advantages and disadvantages of a number of different, commonly used methods and analysis schemes.

The choice of an optimum analysis method may also depend on the type of systems studied. For example, well-localized bonding situations are best described by LMOs, whereas CMOs may be preferable in delocalized situations such as transition-metal complexes and cluster compounds. An approximate relation between orbital energies and optical excitations is typically restricted to CMO treatments. We have recently used the latter type of analysis (with SGO methods) in a study of ^{29}Si chemical shifts in substituted disilenes.[19] Here we will rely more on a localized view, which appeared more natural for the systems studied. CMOs turned out to be less readily interpretable in terms of bonding or antibonding character. An LMO-based analysis for a set of related compounds systems of type $SiMe_nCl_{4-n}$ ($n = 0-4$) has been provided by Berger et al.[20] at the IGLO-HF level. We will mainly concentrate on IGLO-DFT treatments. We will also evaluate NCS analyses, and we will investigate the NBOs of the systems in question.

3. Computational Details

Prior to detailed analyses of the electronic origin of the chemical shifts, we have studied the suitability of molecular models of varying sophistication to correctly represent the structures and chemical shift data of silyllithium compounds obtained in the solid state or in solution. We have furthermore compared different methods for structure optimization and for chemical shift calculations.

All calculations were done without symmetry restrictions. The large amino-substituted silyllithium systems **4**·3THF, **5**·3THF, and **6**·3THF (cf. Figure 6 below) were optimized with the TURBOMOLE[21] program at the B3LYP/TZVP level with starting coordinates taken from the crystal structure analyses.[2,4] All other structure optimizations and harmonic vibrational frequency analyses (to establish the nature of stationary points on the potential energy surface) were performed at the HF/6-31+G(d), B3LYP[22]/6-31+G(d), and MP2/6-31+G(d) levels using the Gaussian 98 program package.[23] Natural population analyses[24] employed the built-in NBO-3.1 subroutines of the Gaussian 98[23] program, whereas NCS[18] analyses of chemical shifts employed the NBO-5.0[25] program. Chemical shifts were initially calculated with Gaussian 98 at the GIAO-HF level,[15,16] using the 6-311+G(2d,p) basis set, while analyses of the individual contributions to shieldings were done at the IGLO-BP86[14] level using the extended Huzinaga/Kutzelnigg basis sets BIII (sometimes termed the IGLO-III basis).[13] In IGLO-BP86 calculations on the large systems **4**·3THF, **5**·3THF, and **6**·3THF a mixed basis was employed, where BIII was used on Si, Li, N, and O and on those carbon atoms directly bonded to silicon and nitrogen, while all other atoms were treated with the smaller Dunning/Huzinaga DZP basis set.[26] For the IGLO-based calculations, the Boys localization[8,27] was used throughout this work. In these calculations, Kohn−Sham orbitals obtained with Gaussian 98 were transferred to the in-house property program MAG-ReSpect,[28] using recently implemented interface routines.[29] Computed absolute shieldings σ were converted to relative shifts δ via calculated shieldings for tetramethylsilane (TMS) obtained at the same levels

(19) Auer, D.; Strohmann, C.; Arbuznikov, A. V.; Kaupp, M. *Organometallics* **2003**, *22*, 2442.
(20) Berger, S.; Bock, W.; Frenking, G.; Jonas, V.; Mueller, F. *J. Am. Chem. Soc.* **1995**, *117*, 3820.
(21) Program System TURBOMOLE V 5.1: Ahlrichs, R.; Baer, M.; Haeser, M.; Horn, H.; Koelmel, C. *Chem. Phys. Lett.* **1989**, *162*, 165.
(22) Lee, C.; Yang, W.; Parr, R. G. *Phys. Rev. B: Condens. Matter* **1988**, *37*, 785. Becke, A. D. *J. Chem. Phys.* **1993**, *98*, 5648.
(23) Frisch, M. J.; Trucks, G. W.; Schlegel, H. B.; Scuseria, G. E.; Robb, M. A.; Cheeseman, J. R.; Zakrzewski, V. G.; Montgomery, J. J. A.; Stratmann, R. E.; Burant, J. C.; Dapprich, S.; Millam, J. M.; Daniels, A. D.; Kudin, K. N.; Strain, M. C.; Farkas, O.; Tomasi, J.; Barone, V.; Cossi, M.; Cammi, R.; Mennucci, B.; Pomelli, C.; Adamo, C.; Clifford, S.; Ochterski, J.; Petersson, G. A.; Ayala, P. Y.; Cui, Q.; Morokuma, K.; Malick, D. K.; Rabuck, A. D.; Raghavachari, K.; Foresman, J. B.; Cioslowski, J.; Ortiz, J. V.; Baboul, A. G.; Stefanov, B. B.; Liu, G.; Liashenko, A.; Piskorz, P.; Komaromi, I.; Gomperts, R.; Martin, R. L.; Fox, D. J.; Keith, T.; Al-Laham, M. A.; Peng, C. Y.; Nanayakkara, A.; Gonzalez, C.; Challacombe, M.; Gill, P. M. W.; Johnson, B.; Chen, W.; Wong, M. W.; Andres, J. L.; Head-Gordon, M.; Replogle, E. S.; Pople, J. A. *Gaussian 98*, revision A.7; Gaussian, Inc.: Pittsburgh, PA, 1998.
(24) (a) Reed, A. E.; Curtiss, L. A.; Weinhold, F. *Chem. Rev.* **1988**, *88*, 899. (b) Reed, A. E.; Weinhold, F. *J. Chem. Phys.* **1985**, *83*, 1736.
(25) Glendening, E. D.; Badenhoop, J. K.; Reed, A. E.; Carpenter, J. E.; Bohmann, J. A.; Morales, C. M.; Weinhold, F. *NBO 5.0*; Theoretical Chemistry Institute, University of Wisconsin, Madison, WI, 2001.
(26) Dunning, T. H.; Hay, P. J. In *Modern Theoretical Chemistry*; Schaefer, H. F., III, Ed.; Plenum: New York, NY, 1976; Vol. 3, p 1.
(27) (a) Edmiston, C.; Ruedenberg, K. *Rev. Mod. Phys.* **1963**, *35*, 457. (b) Edmiston, C.; Ruedenberg, K. *J. Chem. Phys.* **1965**, *43*, 97. (c) Boys, S. F. In *Quantum Theory of Atoms, Molecules and the Solid State*; Löwdin, P. W., Ed.; Academic: New York, NY, 1966; p 253. This procedure is often erroneously attributed to: Foster, J. M.; Boys, S. F. *Rev. Mod. Phys.* **1960**, *32*, 300.
(28) Malkin, V. G.; Malkina, O. L.; Reviakine, R.; Arbuznikov, A. V.; Kaupp, M.; Schimmelpfennig, B.; Malkin, I.; Helgaker, T.; Ruud, K. *MAG-ReSpect*, version 1.1; 2003.
(29) (a) Reviakine, R. *Gaussian-to-MAG interface*, version 1.0; 2002. (b) Kaupp, M.; Reviakine, R.; Malkina, O. L.; Arbuznikov, A.; Schimmelpfennig, B.; Malkin, V. G. *J. Comput. Chem.* **2002**, *23*, 794.

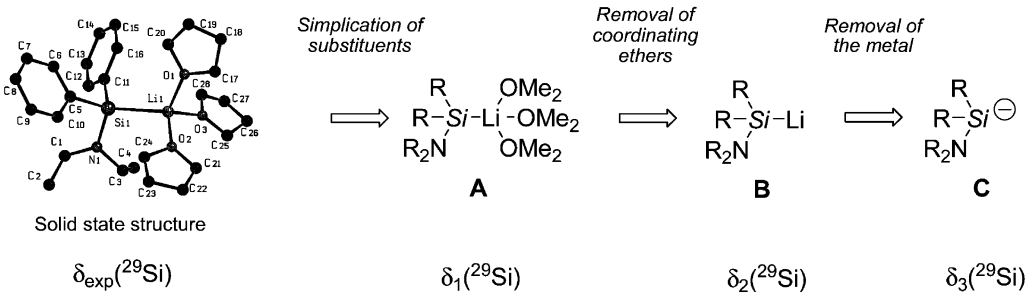

Figure 4. Possible model systems (**A**−**C**) derived from crystal structures of amino-substituted silyllithiums.

[σ_{calcd}(Si) = 385.9 ppm for GIAO-HF/6-311+G(2d,p)//B3LYP/6-31+G(d) and 332.0 ppm for IGLO-BP86/BIII//B3LYP/6-31+G(d)].

4. Results and Discussion

Before closer analysis of the chemical shifts, suitable model systems and quantum-chemical methods had to be selected (see above), based on the following questions: (a) Which methods and basis sets are required for a proper description of structure and chemical shifts in lithiated silanes? (b) Which simplifications in the model system are possible on the silicon side (e.g. reduction of substituents) and on the lithium side (e.g. simplification or removal of coordinating ether molecules, removal of the metal) to maintain sufficiently accurate NMR chemical shifts for a detailed interpretation?

With the solid-state structure of a dialkylamino-substituted silyllithium compound as the starting point, typically the first simplification was (a) replacement of the hydrocarbon rings or chains on silicon and heteroatoms by methyl groups (*simplification of substituents*), leading to a system of type **A** (Figure 4). Further reductions are possible (b) by *removal of coordinating ethers* to give the unsolvated silyllithium model **B**, and (c) by *removal of the metal*, leading to the silyl anion **C**.

4.1. Structure Optimization. Quantum-chemical methods and basis sets were tested on the structures of trimethyl-substituted models **1**−**3** (Figure 5; see Table 1 in the Supporting Information for the optimized structural parameters of **1**−**3**). Since the main part of this work deals with the chemical shifts of heteroatom-substituted silanes, it is desirable to obtain reasonably accurate structures with simplified models.

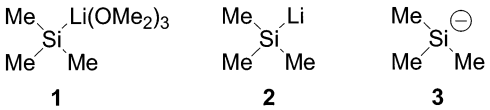

1 **2** **3**

Figure 5. Model systems **1**−**3** compared for silyllithium compounds.

Inclusion of electron correlation (e.g. by MP2 or DFT methods) is required for a sufficient description of certain structural parameters, especially angles at the heteroatoms connected to the silicon center. The closely related Si−O−Si bond angles in neutral siloxane systems, for example, are not described correctly at the Hartree−Fock level (HF).[30] Studies on compounds of type $SiMe_nCl_{4-n}$ ($n = 0-4$) by Berger et al. indicate also the need for correlated methods in structure optimization.[20] In view of its good cost/performance ratio, DFT with the B3LYP hybrid functional turned out to be the method of choice for all model systems, giving close agreement to experimental structures (see Table 1 in the Supporting Information for detailed structure discussions of models **1**−**3**).

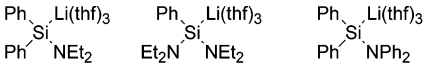

4·3 THF **5**·3 THF **6**·3 THF

Figure 6. Amino-substituted silyllithium compounds **4**·3THF, **5**·3THF, and **6**·3THF with known solid-state structures.[2,4]

4.2. Comparison of Structural Models. *Removal of coordinating ethers* (Figure 4) results in a contraction of the Si−Li bond length in model **2** compared to that in **1**. As a further consequence, the Si−C bond lengths are also reduced while the C−Si−C angles increase (see Table 1 in the Supporting Information for details). For the free gas-phase anion **3**, bond lengths and angles change again significantly (partly due to rehybridization at silicon) and do thus not reproduce sufficiently the structural parameters of a solvated silyllithium complex. It is furthermore known experimentally that the influence of the metal on the ^{29}Si chemical shift of silylmetal compounds is appreciable.[31] Therefore, the type **C** model **3** has to be dismissed, leaving the question open as to whether systems of type **B**, such as **2**, are suitable for the description of qualitative changes of the chemical shift.

To answer this question, the entire THF-coordinated systems **4**·3THF, **5**·3THF, and **6**·3THF (Figure 6; starting coordinates were taken from the solid-state structures[2,4]) were optimized (see Table 1 for selected bond lengths and angles and Tables 13−15 in the Supporting Information for standard orientations).

Comparison of calculated with experimental solid-state structural results for **4**·3THF, **5**·3THF, and **6**·3THF reveals that almost all Si−Li and Si−N bond lengths are slightly overestimated by the calculation, while the angles around the silicon and nitrogen centers are reproduced well (see Table 1). After removal of the THF solvent molecules, model systems **4**−**6** were optimized at the B3LYP/6-31+G(d) level (Figure 7). The characteristic trends for bond lengths and angles are reproduced at this level (Table 1), but with Si−Li bonds that are significantly too short.

(30) Corminboeuf, C.; Heine, T.; Weber, J. *Chem. Phys. Lett.* **2002**, *357*, 1 and references cited therein.

(31) Kayser, C.; Fischer, R.; Baumgartner, J.; Marschner, C. *Organometallics* **2002**, *21*, 1023 and references cited therein.

Table 1. Selected Experimental and Calculated Structure Parameters and ^{29}Si Chemical Shifts of Lithiosilanes 4−6

	exptl values[a]			calcd values[b]					
param	**4**·3THF[2]	**5**·3THF[2]	**6**·3THF[4]	**4**·3THF	**5**·3THF	**6**·3THF	**4**	**5**	**6**
Si−Li (pm)	268.2(8)/267.8(8)	262.7(4)	273.2(7)	270.3	270.0	272.4	249.1	248.5	248.9
Si−N (pm)	176.4(4)/176.3(4)	178.1(2)/177.2(2)	182.4(3)	181.2	182.8/181.7	186.4	178.7	179.1/178.8	187.4
C−Si−C (deg)	100.1(2)/99.7(2)		105.4(1)	101.7		105.9	104.3		106.4
N−Si−N (deg)		112.66(11)			111.7			114.3	
N (sum of angles) (deg)	357.6/354.1	354.9/358	360.0	355.2	355.8/358.8	360.0	355.0	356.7/359.8	359.7
δ(^{29}Si) (ppm)	20.3	28.4	10.6/10.8[c]	23.7[d] (27.4)	36.1[d] (38.2)	19.1[d] (16.6)	21.0[d] (27.4)	24.6[d] (26.5)	23.2[d] (26.3)

[a] See refs 2 and 4 for details on the crystal structure analyses of **4**·3THF, **5**·3THF, and **6**·3THF; **4**·3THF has two independent molecules in the asymmetric unit. [b] **4**·3THF, **5**·3THF, and **6**·3THF were optimized at the B3LYP/TZVP level and **4**−**6** at the B3LYP/6-31+G(d) level. [c] The authors cite two different values in the original work (see ref 4). [d] Calculated chemical shifts relative to TMS at the GIAO-HF/6-311+G(2d,p) level (shifts at the IGLO-BP86/BIII level are given in parentheses) for **4**·3THF, **5**·3THF, and **6**·3THF mixed basis sets were used (see Computational Details).

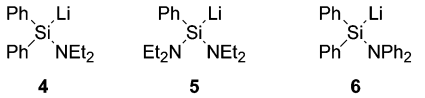

Figure 7. Model systems **4**−**6** compared for amino-substituted silyllithium compounds.

4.3. Model and Structure Dependence of Chemical Shifts. The ^{29}Si chemical shifts of all models **4**−**6** (cf. Figures 6 and 7) with and without the THF coordination sphere were calculated at the GIAO-HF/6-311+G(2d,p) level. The results agree within 1−13 ppm to experimental values. Fortuitously, the data for type **B** models **4** and **5** were closer to experiment than those for type **A** models **4**·3THF and **5**·3THF. This may arise from further solvent effects, from neglect of conformational averaging, and from other error compensation. As we are mainly interested here in a qualitative understanding of substituent effects on ^{29}Si shifts, we believe that the nonsolvated type **B** models are adequate for our purpose. The experimentally observed trends are furthermore reproduced also at the IGLO-BP86/BIII level used for the detailed interpretations (see Table 2).

The main substituted model systems of interest were methoxy-, dimethylamino-, and methylthio-substituted silanes of types **D**−**F** (Figure 8). Since substituents of type Y (Y = OMe, SMe, NMe_2) are not symmetrical toward rotation around the Si−Y bond, almost all molecules have several conformers, which are expected to differ in energy and ^{29}Si chemical shifts. Therefore, a systematic treatment of conformers had to be found.

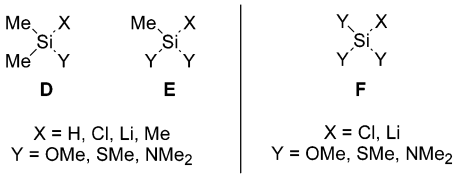

Figure 8. Model systems **D**−**F** compared for heteroatom-substituted silanes.

With a B3LYP/6-31+G(d) optimized structure as the starting point (as an example, see (MeO)Me_2SiCl (**7**) in Figure 9), the C−Y−Si−X dihedral angle (X = H, Cl, Li, Me; Y = O, N, S) was varied in steps of 60° to give various starting structures. After preoptimization[32] and rejection of equivalent stationary points, all structures were fully B3LYP/6-31+G(d) optimized. For all nonidentical minima, the ^{29}Si chemical shifts were calculated at the GIAO-HF/6-311+G(2d,p), IGLO-BP86/BIII, and SGO-BP86/BIII levels (absolute isotropic shielding values for IGLO-BP86/BIII are given in Table 2; GIAO-HF/6-311+G(2d,p) and SGO-BP86/BIII results are given in Tables 2 and 3 in the Supporting Information). The obtained isotropic ^{29}Si shieldings may depend appreciably on conformation. For consistency, we carried out our analyses only for models with closely corresponding conformations.[33] Where this is not an absolute minimum, the shift results are marked in Table 2.[34] Structure optimizations for $(MeS)_3SiCl$ and $(MeS)_3SiLi$ started from chosen conformations of $(MeO)_3SiCl$ and $(MeO)_3SiLi$, respectively. In view of the energetic similarity of

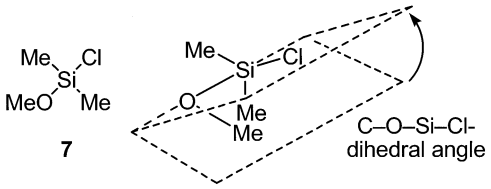

Figure 9. Lewis structure of the methoxy-substituted model **7** (left side) and illustration of the dihedral angle in this heteroatom-substituted model (right side).

Table 2. Calculated ^{29}Si Nuclear Shieldings σ (ppm) for the Models $Y_nMe_{3-n}SiX$ (n = 0−3)[a]

		σ			
model	Y	X = H	X = Cl	X = Li	X = Me
Me_3SiX		349.9	292.4	341.7	332.0
$(Y)Me_2SiX$	OMe	323.5	310.2	276.1	312.3
	NMe_2	341.6[b]	314.7	298.3	326.4
	SMe	326.3	284.4	302.1[b]	311.5
$(Y)_2MeSiX$	OMe	345.8	351.1[b]	287.0	333.1
	NMe_2	347.3	338.2	291.0	337.3
	SMe	314.5	279.6	287.8	294.2
$(Y)_3SiX$	OMe		400.6[b]	341.3[b]	
	NMe_2		362.2	323.2[b]	
	SMe		280.8[c]	266.8[c]	

[a] IGLO-BP86/BIII//B3LYP/6-31+G(d) results. [b] Values from local minimum structure. [c] Optimization started from a conformationally identical model as the local minimum of the corresponding $(MeO)_3SiX$ system.

(32) In principle 6 different starting structures for monosubstituted, 36 for bis-substituted, and 216 for tris-substituted silanes are imaginable, but due to reasons of symmetry and identity the total amount of different starting structures is lower. After this selection all remaining structures were optimized at the lower HF/3-21G (X = H, Me, Cl) and HF/3-21G* (X = Li) levels.

(33) Unfortunately for models of the types $(Y)_2MeSiX$ and $(Y)_3SiX$ (X = Cl, Li; Y = OMe, NMe_2, SMe) not all structures correspond exactly in conformation. Thus, the model with the smallest deviations from the others was used.

various conformers, a more quantitative evaluation of the shieldings would require Boltzmann averaging. However, the important trends we intend to analyze are reproduced by the chosen minima.

Note that, for a given substitution pattern, the charge at the silicon center is always more positive for the chlorosilane than for the corresponding lithiosilane (cf. computed NPA charges in Table 190 of the Supporting Information). It is thus clear that the charge at the silicon center alone cannot explain the observed and computed trends.

4.4. IGLO-LMO Analyses. The LMO analyses of the IGLO-BP86 calculations show that the dominant contributions to shielding originate generally from the LMOs of the four σ-bonds to silicon. Only in a few situations do further contributions from the lone pairs (LP) of the heteroatoms O, N, and S become significant. For clarity of presentation, the LP contributions on all O, N, or S substituents were added up ($\sum$LP(Y)). Contributions by all core-type LMOs on silicon are also summed up ($\sum$core(Si)).

Me_3SiX Systems. In a previous study, Berger et al. analyzed the ^{29}Si shielding for systems of type $SiMe_nCl_{4-n}$ ($n = 0-4$) in terms of bonding LMOs at the HF level.[20] This analysis will be extended here. We start with the simplest systems of type Me_3SiX. The largest deshielding in Me_3SiCl originates from the three Si−C bonding LMOs, while the Si−Cl bonding LMO contributes significantly less (Table 3). Me_3SiLi differs from this, since the Si−C LMOs contribute much less, and now the largest individual contribution arises from the Si−Li bonding orbital (Table 3). Due to the less deshielding Si−C contributions, an overall larger shielding results for Me_3SiLi than for Me_3SiCl, in agreement with experimental observation (see also Figure 2; experimental ^{29}Si NMR results Me_3SiCl (THF) at δ 29.8;[35a] Me_3SiLi (THF-d_8) at δ −32.2[35b]).

Table 3. Analysis of Major LMO Contributions to σ(^{29}Si) for Me_3SiX[a]

contribn to σ	X = Cl	X = Li
total	+292.4	+341.7
$\sum$core(Si)	+786.5	+779.8
Si−C (3×)	−137.4	−107.0
Si−X	−78.1	−113.5

[a] IGLO-BP86/BIII//B3LYP/6-31+G(d) results.

(Y)Me_2SiX Systems (Model D). Introduction of an electron-withdrawing group alters the bonding around the silicon center, and thus the chemical shifts, appreciably. For all three substituted chlorosilane systems the contributions by Si−C and Si−Cl LMOs are enhanced (more negative) compared to Me_3SiCl, to varying extents. The Si−C and Si−Cl contributions in (MeS)-Me_2SiCl are somewhat larger than in $(Me_2N)Me_2SiCl$ (Table 4). The overall larger shielding compared to Me_3SiCl is due to the replacement of a more deshielding Si−C by a less deshielding Si−Y contribution. This is less pronounced for the Si−S LMO contribution in the methylthio-substituted system.

Table 4. Analysis of the Major LMO Contributions to σ(^{29}Si) for (Y)Me_2SiX[a]

Y	contribn to σ	X = Cl	X = Li
OMe	total	+310.2	+276.1
	$\sum$core(Si)	+796.0	+784.4
	Si−C	−148.1	−134.0
	Si−C	−149.5	−134.5
	Si−O	−97.3	−90.0
	Si−X	−91.4	−155.0
	$\sum$LP(O)	+11.8	+13.2
NMe_2	total	+314.7	+298.3
	$\sum$core(Si)	+791.6	+781.3
	Si−C	−139.5	−119.4
	Si−C	−139.4	−120.2
	Si−N	−95.3	−104.3
	Si−X	−82.4	−134.4
	$\sum$LP(N)	−11.0	+4.8
SMe	total	+284.4	+302.1
	$\sum$core(Si)	+788.1	+778.1
	Si−C	−142.9	−126.0
	Si−C	−143.6	−121.1
	Si−S	−121.6	−85.2
	Si−X	−88.4	−134.7
	$\sum$LP(S)	−4.3	−3.1

[a] IGLO-BP86/BIII//B3LYP/6-31+G(d) results.

In monosubstituted lithiosilane systems the Si−C LMO contributions become also significantly more deshielding compared to that in Me_3SiLi. Again, the effect is larger for $(MeS)Me_2SiLi$ than for $(Me_2N)Me_2SiLi$ but is largest for $(MeO)Me_2SiLi$. Additional, particularly large deshielding comes from the Si−Li LMO in all three cases. The Si−Y bonding LMO contributions are largest for $(Me_2N)Me_2SiLi$ and lower for the two other cases (Table 4; see below for explanations). For $(MeO)Me_2SiLi$ and $(Me_2N)Me_2SiLi$, the increased Si−Li LMO contributions overcompensate the replacement of one Si−C contribution by a less deshielding Si−Y contribution, and overall greater deshielding than in Me_3SiLi or than in the corresponding chlorosilanes is found. In contrast, the chlorosilane remains more deshielded for the methylthio-substituted models, due to the effect of the occupied Si−S LMO (explanation see also 4.6).

(Y)$_2$MeSiX Systems (Model E). Replacement of a second methyl group by a methoxy, dimethylamino, or methylthio substituent enhances further several deshielding LMO contributions (Table 5). The trends are similar to those for the monosubstituted silanes, and we thus mention only the differences. When a disubstituted system is compared with its corresponding monosubstituted silane, the deshielding of almost each LMO is once again enhanced, with the exception of the Si−C LMO in $(MeO)_2MeSiCl$ and the Si−N LMOs in $(Me_2N)_2MeSiX$ (X = Cl, Li). However, due to the replacement of a more deshielding Si−C contribution by a less deshielding Si−Y (Y = O, N) contribution, overall enhanced shielding is observed for $(MeO)_2MeSiX$ (X = Cl, Li) and for $(Me_2N)_2MeSiCl$ (compared to the monosubstituted systems). The methylthio-substituted $(MeS)_2MeSiX$ (X = Cl, Li) remains again an exception (cf.

(34) Total energies of these relative minimum structures are within a range of 0.53−5.93 kJ higher than their corresponding absolute minimum. The difference in ^{29}Si shielding for GIAO ($\Delta\sigma_{GIAO}$) and IGLO ($\Delta\sigma_{IGLO}$) calculated systems is determined by subtraction of the shielding of the absolute minimum from that of the relative minimum. $(Me_2N)Me_2SiH$: ΔE = 0.53 kJ, $\Delta\sigma_{GIAO}$ = +4.2, $\Delta\sigma_{IGLO}$ = +5.1. $(MeS)Me_2SiLi$: ΔE = 4.95 kJ, $\Delta\sigma_{GIAO}$ = −12.5, $\Delta\sigma_{IGLO}$ = −20.4. $(MeO)_2MeSiCl$: ΔE = 5.93 kJ, $\Delta\sigma_{GIAO}$ = −4.3, $\Delta\sigma_{IGLO}$ = −8.2. $(MeO)_3SiCl$: ΔE = 4.93 kJ, $\Delta\sigma_{GIAO}$ = −2.4, $\Delta\sigma_{IGLO}$ = −4.0. $(MeO)_3SiLi$: ΔE = 1.79 kJ, $\Delta\sigma_{GIAO}$ = −8.2, $\Delta\sigma_{IGLO}$ = −11.1. $(Me_2N)_3SiLi$: ΔE = 5.23 kJ, $\Delta\sigma_{GIAO}$ = +10.2, $\Delta\sigma_{IGLO}$ = +12.7.

(35) (a) Olah, G. A.; Hunadi, R. J. *J. Am. Chem. Soc.* **1980**, *102*, 6989−6992 and references cited therein. (b) Nanjo, M.; Sekiguchi, A.; Sakurai, H. *Bull. Chem. Soc. Jpn.* **1998**, *71*, 741−747.

Table 5. Analysis of the Major LMO Contributions $\sigma(^{29}Si)$ for $(Y)_2MeSiX$[a]

Y	contribn to σ	X = Cl	X = Li
OMe	total	+351.1	+287.0
	∑core(Si)	+805.2	+794.2
	Si−C	−146.0	−150.8
	Si−O	−112.4	−94.3
	Si−O	−97.4	−101.2
	Si−X	−103.2	−171.6
	∑LP(O)	+20.8	+22.8
NMe_2	total	+338.2	+291.0
	∑core(Si)	+796.8	+785.1
	Si−C	−140.1	−130.8
	Si−N	−90.3	−105.2
	Si−N	−91.2	−85.0
	Si−X	−87.2	−151.5
	∑LP(N)	−34.8	−5.0
SMe	total	+279.6	+287.8
	∑core(Si)	+789.7	+781.5
	Si−C	−146.8	−133.3
	Si−S	−127.4	−106.5
	Si−S	−132.8	−102.3
	Si−X	−97.9	−137.3
	∑LP(S)	−4.8	−7.5

[a] IGLO-BP86/BIII//B3LYP/6-31+G(d) results.

Table 6. Analysis of the Major LMO Contributions to $\sigma(^{29}Si)$ for $(Y)_3SiX$[a]

Y	contribn to σ	X = Cl	X = Li
OMe	total	+400.6	+341.3
	∑core(Si)	+813.4	+803.9
	Si−O	−103.3	−90.8
	Si−O	−112.5	−104.8
	Si−O	−97.3	−107.5
	Si−X	−102.5	−161.1
	∑LP(O)	+23.3	+18.3
NMe_2	total	+362.2	+323.2
	∑core(Si)	+797.7	+787.6
	Si−N	−55.4	−67.7
	Si−N	−83.3	−68.2
	Si−N	−63.2	−66.6
	Si−X	−84.6	−153.8
	∑LP(N)	−127.2	−84.4
SMe	total	+280.8	+266.8
	∑core(Si)	+791.2	+784.2
	Si−S	−134.8	−119.7
	Si−S	−134.3	−115.1
	Si−S	−135.5	−121.9
	Si−X	−103.8	−141.4
	∑LP(S)	−3.4	−13.5

[a] IGLO-BP86/BIII//B3LYP/6-31+G(d) results.

below). The general analysis is additionally complicated by nonnegligible contributions from lone pairs at the heteroatomic substituents. These contributions may be either appreciably shielding, as for the dimethoxy-substituted systems, or deshielding, as in $(Me_2N)_2$-MeSiCl. For the methoxy- and dimethylamino-substituted cases, the difference in shielding between chloro- and lithiosilane systems increases with the introduction of a second heteroatomic substituent, consistent with experiment (cf. Figure 2). This is due to the dominance of the aforementioned replacement of a more deshielding Si−C by a less deshielding Si−Y contribution for the chlorosilanes, while the dramatically enhanced Si−Li contribution leads to great deshielding in $(MeO)_2$-MeSiLi and $(Me_2N)_2$MeSiLi (Table 5). Differences remain much smaller with methylthio substituents, where the Si−S LMOs play again a somewhat different role (see also 4.6).

$(Y)_3SiX$ Systems (Model F). The replacement of the last methyl group by a heteroatomic substituent still has an appreciable influence (Table 6). The now overall increased shieldings in $(MeO)_3SiX$ and $(Me_2N)_3SiX$ (X = Cl, Li), and in $(MeS)_3SiLi$ are due to the significantly lower deshielding contributions by Si−Y LMOs compared to those by Si−C LMOs, as mentioned above. These are no longer compensated by enhanced individual contributions, and thus the shielding increases overall. This effect is more pronounced for the chlorosilanes, and thus the differences between chlorosilanes and lithiosilanes are further enhanced. In $(MeS)_3SiCl$, the changes in individual contributions are small and of opposite direction, such that the overall shielding remains almost unchanged. The overall still large deshielding Si−S contributions make the methylthio-substituted systems the most deshielded cases by far.

Further contributions come again from the substituent lone pairs in methoxy- and dimethylamino-functionalized models. The unrealistically large deshielding LP contributions for the amino-substituted systems (Table 6) indicate a problem with the Boys localization, as the Si−N LMO contributions are simultaneously reduced significantly. It seems that a large mixing of the two types of LMOs makes the analysis of the Si−N and ∑LP(N) contributions unreliable in these cases.

4.5. Comparison of IGLO-LMO and NCS-NBO-(NLMO) Results: Shielding Tensors for Me_3SiX. As an analysis of the nuclear shieldings in terms of strictly localized NBOs was hoped to provide additional insights, we have also evaluated Weinhold's NCS analysis[18] for the simplest models Me_3SiX (X = Cl, Li). Tables 7 and 8 compare the IGLO-LMO and GIAO-NCS analyses, respectively, for the ^{29}Si shielding tensors of both systems. As both molecules have axial symmetry, we provide the results in terms of $\sigma_{||}$ and $\sigma_{\perp}$ components and sum up the three symmetrically equivalent Si−C contributions. In the NCS analyses, the principal NBO contributions and delocalization tails have furthermore

Table 7. IGLO Analysis of the Major LMO Contributions to $\sigma(^{29}Si)$ Tensors for Me_3SiX[a]

model	contribn to	$\sigma_{\perp}$	$\sigma_{||}$	σ_{iso}
Me_3SiCl	total	+281.9	+313.5	+292.4
	∑core(Si)	+789.9	+779.8	+786.5
	3 Si−C	−378.1	−480.8	−412.3
	Si−Cl	−119.8	+5.3	−78.1
Me_3SiLi	total	+335.1	+355.1	+341.7
	∑core(Si)	+774.4	+790.3	+779.8
	3 Si−C	−265.9	−431.3	−321.0
	Si−Li	−175.6	+10.6	−113.5

[a] IGLO-BP86/BIII//B3LYP/6-31+G(d) results.

Table 8. NCS Analysis of the Major NLMO Contributions to $\sigma(^{29}Si)$ Tensors for Me_3SiX[a]

model	contribn to	$\sigma_{\perp}$	$\sigma_{||}$	σ_{iso}
Me_3SiCl	total	+277.4	+306.9	+287.3
	∑core(Si)	+596.7	+580.0	+591.1
	3 Si−C	−226.7	−271.7	−241.7
	Si−Cl	−64.9	+4.7	−41.7
Me_3SiLi	total	+332.9	+350.6	+338.8
	∑core(Si)	+637.7	+600.7	+625.4
	3 Si−C	−137.4	−239.3	−171.3
	Si−Li	−152.7	+9.3	−98.7

[a] GIAO-BP86/BIII//B3LYP/6-31+G(d) results.

been summed up, so that the entries correspond to contributions from NLMOs.

One might expect that the two types of analyses will provide very similar interpretations. This holds true for several of the main features: (a) the Si−C bonding orbitals are responsible for the main deshielding, (b) the Si−Li contribution in Me_3SiLi is much more deshielding than the Si−Cl contribution in Me_3SiCl, (c) the Si−X contributions are only deshielding for $\sigma_\perp$, and (d) the Si−C bonding orbitals contribute more to $\sigma_\parallel$ than to $\sigma_\perp$. However, there are also notable differences: the NCS analysis provides considerably less positive core−shell contributions than the IGLO-LMO treatment. Consequently, the valence-shell contributions are much more negative in the latter than in the former case (the overall shieldings obtained at the underlying GIAO-BP86 and IGLO-BP86 levels differ very little). The most striking observation is the lack of conservation of the core−shell contributions in the NCS analyses. While the 1s core−shell contributions for first-row main-group nuclei were constant in a previous study,[18] and the silicon 1s-shell contributions are also transferable here, the 2s/2p-shell contributions increase by more than 30 ppm on going from X = Cl to X = Li, while differences at the IGLO-LMO level are below 7 ppm. This renders the NCS analysis less useful in the present study.

4.6. Further Interpretation: NBO Analyses. Despite this weakness of the NBO-based NCS analysis we will in the following make use of implicit information from NBO analyses in the further discussion of substituent effects on ^{29}Si shieldings. While the IGLO-LMO analyses allow in principle a further breakdown of σ^p into contributions from individual terms ("excitations") in the sum-over-states expansion of the UDFT calculations (cf. eq 2), the virtual orbitals involved are canonical, delocalized MOs. This renders a "localized" description more difficult. As closer inspection of NBOs and NLMOs obtained reveals close similarity to the LMOs obtained in the Boys localization, we may extend our understanding of the origin of substituent effects on shieldings by inspection of "bonding" and "antibonding" NBOs. We will use the approximate shape and energies of NBOs to qualitatively interpret the trends found in the occupied LMO contributions in section 4.4.

Analyses of Si−X, Si−Y, and Si−C bonding NBOs in model systems of types **D**−**F** confirm an increasing polarization of the bond away from silicon with increasing substituent electronegativity, roughly along the series Si−Li ≪ Si−S < Si−C < Si−N < Si−Cl < Si−O. Notably, the sequence is reversed for the corresponding antibonding NBOs. The PSO matrix element in eq 2 (second matrix element), which involves the electron−nucleus distance to the third power in the denominator, is extremely sensitive to the charge distribution around silicon. From an overlap point of view, we expect that the PSO matrix element will be largest for a coupling between an Si−Li bonding and an Si−O antibonding orbital (Figure 10, top), smallest for a coupling between an Si−O bonding and an Si−Li antibonding orbital (Figure 10, bottom), and intermediate for other combinations of bonding and antibonding localized orbitals around silicon. These trends will be reflected in the paramagnetic shielding contribution of a particular term in the sum-over-states expansion. In addition, we have to consider the energy denominators in eq 2. That is, the individual couplings will contribute most when the energy of the bonding orbital is relatively high and that of the antibonding orbital that couples to it is low. With these arguments in mind, we may rationalize our findings in section 4.4.

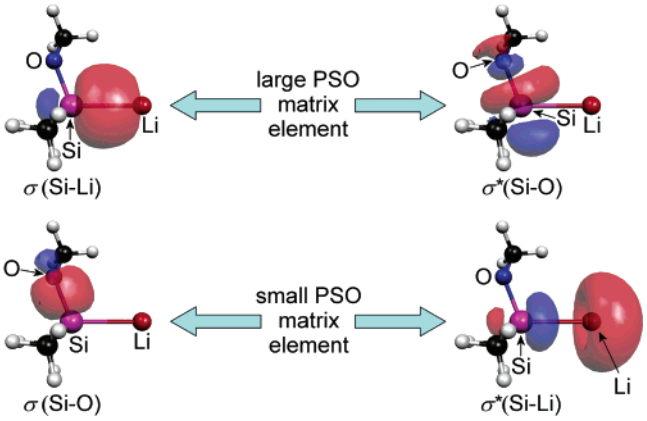

Figure 10. Interpretation of coupling between σ(Si−Li) and σ^*(Si−O) (top) as well as between σ(Si−O) and σ^*(Si−Li) (bottom) orbitals.[36]

In chlorosilanes the introduction of heteroatomic substituents increases deshielding contributions by Si−C LMOs due to the large couplings of σ(Si−C) to σ^*(Si−Y) orbitals, both of which have large coefficients at silicon. The influence by the Si−Cl bond increases as well but remains smaller overall, due to the polarization of this orbital toward the electronegative chlorine substituent. Contributions by Si−O and Si−N bonding orbitals are also relatively small due to their polarization away from silicon. With an increasing number of substituents Y, there is thus a competition between the increased Si−C contributions and the fact that their number decreases (they are replaced by the much less deshielding Si−Y contributions). This leads to an overall nonmonotonic behavior, as has been found previously for the $SiMe_nCl_{4-n}$ (n = 0−4) series.[20] The Si−S bonds exhibit larger Si character and are higher in energy, and they therefore contribute more. This distinguishes the methylthio-substituted systems from the methoxy- or dimethylamino-substituted cases.

The situation becomes more complicated when going to the lithiosilanes. The Si−Li bond is not only polarized strongly toward silicon but corresponds also to an energetically high-lying orbital (in the CMO framework, it tends to correspond to the HOMO, leading to a smaller HOMO−LUMO gap than in the chlorosilanes). The Si−Li LMO contributions in section 4.4 were thus particularly deshielding. Moreover, they became consecutively more deshielding with the introduction of further electronegative substituents Y, due to large couplings of the type σ(Si−Li)→σ^*(Si−Y). This explains to a great extent why the substituted lithiosilanes tend to exhibit much lower shielding than their chlorosilane analogues, increasingly so with successive substitution (despite low Si−Y contributions).

(36) (a) Flükiger, P.; Lüthi, H. P.; Portmann, S.; Weber, J. *MOLEKEL 4.3*, Swiss Center for Scientific Computing, Manno, Switzerland, 2000−2002. (b) Portmann, S.; Lüthi, H. P. *Chimia* **2000**, *54*, 766.

5. Conclusions

Introduction of electronegative substituents into a chloro- or lithiosilane has a profound influence on the electronic situation around silicon and thus on the ^{29}Si NMR chemical shifts. While Me_3SiCl has a larger shift than Me_3SiLi, this trend is reversed in the heteroatom-substituted compounds. This different behavior of chloro- and lithiosilanes may not be understood from oversimplified arguments based on the charge on silicon. Instead, it is the simultaneous presence of electronegative and electropositive substituents that leads to the large shifts in substituted lithiosilanes, due to large couplings between occupied and unoccupied orbitals with significant silicon character and relatively small energy differences. Methylthio substituents behave somewhat differently than methoxy or dimethylamino substituents, due to their inherently lower electronegativity and the typically smaller energy denominators involved. By the presented results the "unexpected" ^{29}Si NMR shifts in heteroatom-substituted silyllithium compounds become comprehensible, and thus they are important probes for research groups doing experimental work.

Acknowledgment. This study has been supported by the Deutsche Forschungsgemeinschaft and via the Graduiertenkolleg 690 "Electron Density: Theory and Experiment" at Universität Würzburg, by the Fonds der Chemischen Industrie, and by Wacker-Chemie GmbH. We are grateful to A. V. Arbuznikov for technical assistance.

Supporting Information Available: Tables including the standard orientation and the total energies of model systems **1**−**6** and of all evaluated type **D**−**F** models, calculated shielding tensors for Si (GIAO/IGLO) and the MO contributions to σ (IGLO) for these models. Further tables give information on the NBO analysis for the bonds to silicon in selected chlorosilane and silyllithium model systems. This material is available free of charge via the Internet at http://pubs.acs.org.

OM049812K